Ab initio electron-defect interactions using Wannier functions

Supplementary Information

I-Te Lu,[1] Jinsoo Park,[1] Jin-Jian Zhou,[1] and Marco Bernardi*,[1]

[1] *Department of Applied Physics and Materials Science, California Institute of Technology, Pasadena, California 91125*

* *bmarco@caltech.edu*

EFFECT OF THE DEFECT POSITION AND WIGNER-SEITZ SUPERCELL SIZE ON THE INTERPOLATED MATRIX ELEMENTS

The DFT supercell used to obtain the perturbation potential is not equivalent to the Wigner-Seitz (WS) supercell used to construct the WFs (see Supplementary Figure 1a). The size of the WS supercell is equal to the size of the BZ coarse grid, and does not depend on the size of the DFT supercell. Let the lattice vector $\boldsymbol{R}_{\mathrm{d}}$ be the location of the unit cell containing the defect within the DFT supercell. The lattice vector $\boldsymbol{R}_{\mathrm{d}}$ can lie outside the WS supercell if the latter is not large enough to enclose the perturbation potential (see Supplementary Figure 1a). This scenario should be avoided as it leads to large interpolation errors. To include the perturbation potential in the WS supercell, we move the lattice point $\boldsymbol{R}_{\mathrm{d}}$ to the origin of the WS supercell; using a well-known property of the Fourier transform, we multiply the e-d matrix elements computed using the DFT supercell by the phase factor $e^{i(\boldsymbol{k}'-\boldsymbol{k})\cdot\boldsymbol{R}_{\mathrm{d}}}$; the resulting e-d matrix elements correctly take into account the translation of the defect site, and can be used in the e-d interpolation procedure.

To verify the accuracy of this approach, we define and compute an invariant e-d coupling, $M_{\mathrm{inv}}(\boldsymbol{k}', \boldsymbol{k})$, as

$$M_{\mathrm{inv}}(\boldsymbol{k}', \boldsymbol{k}) = \sqrt{\sum_{mn} |M_{mn}(\boldsymbol{k}', \boldsymbol{k})|^2}, \tag{S1}$$

which is invariant under the operation of the fine-grid unitary matrix $U_{\boldsymbol{k}_{\mathrm{f}}}$ used to interpolate e-d matrix elements. The invariant e-d coupling computed from the interpolated matrix elements depends on the defect-site lattice vector $\boldsymbol{R}_{\mathrm{d}}$ through the e-d matrix elements in the Wanniner representation [see Eq. (5)]. Supplementary Figure 1b shows how the choice of the defect-site lattice vector $\boldsymbol{R}_{\mathrm{d}}$ affects the invariant e-d coupling $M_{\mathrm{inv}}(\boldsymbol{k}', \boldsymbol{k})$. To this end, we interpolate the e-d matrix elements starting from a coarse $10 \times 10 \times 10$ BZ grid. When the defect is placed at the lattice vector $\boldsymbol{R}_{\mathrm{d}} = (3, 3, 3)$ (in Bravais lattice vector units), the interpolated e-d matrix elements deviate significantly from the directly computed ones because the perturbation potential lies outside the WS supercell. We can improve the interpolated results by moving the lattice point $\boldsymbol{R}_{\mathrm{d}}$ to the origin of the WS supercell, and multiplying the matrix elements by a phase factor, as discussed above. Using this approach, the interpolated e-d matrix elements are in excellent agreement with the directly computed ones, as is shown in the $\boldsymbol{R}_{\mathrm{d}} = \boldsymbol{0}$ curve in Supplementary Figure 1b. All the results in this work have been obtained by moving the defect-site lattice vector $\boldsymbol{R}_{\mathrm{d}}$ to

the origin of the WS supercell after computing the e-d matrix elements on the coarse BZ grid.

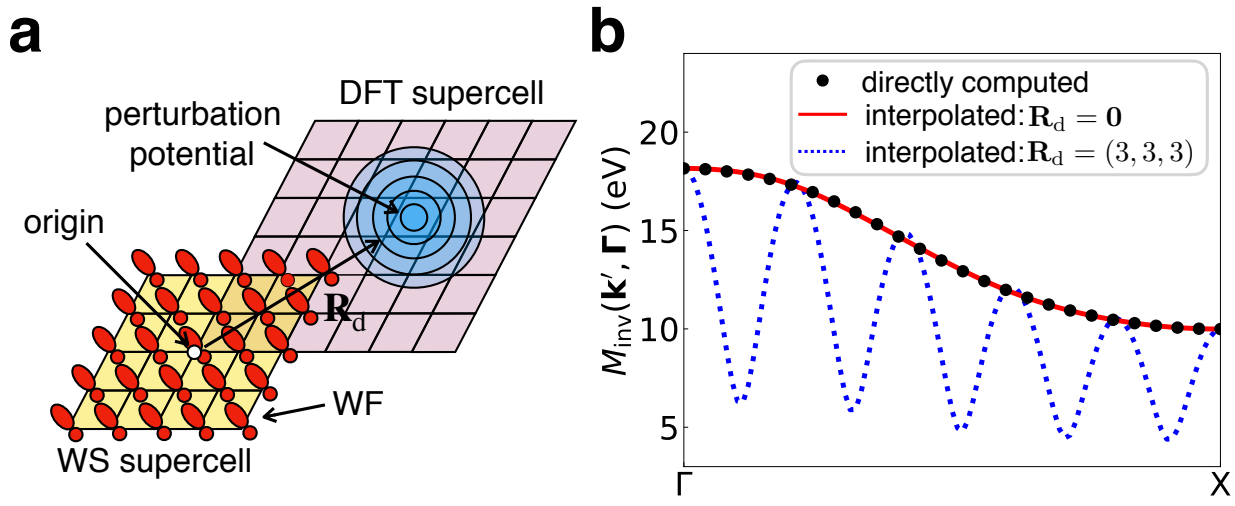

Supplementary Figure 1. Supercells and matrix elements. **a** Schematic of the DFT and WS supercells. **b** Effect of the defect position $\boldsymbol{R}_\mathrm{d}$ on the invariant e-d coupling $M_\mathrm{inv}(\boldsymbol{k}', \boldsymbol{k})$. The interpolated e-d matrix elements are computed starting from a coarse $10 \times 10 \times 10$ BZ grid. The crystal momentum of the initial state is set to the $\mathbf{\Gamma}$ point, and the crystal momentum $\boldsymbol{k}'$ of the final state is varied along the high-symmetry BZ line shown in figure.

SCATTERING STRENGTH IN COPPER AND SILICON

We compute the scattering strength $|M(\varepsilon_{n\boldsymbol{k}})|$ for carrier energy $\varepsilon_{n\boldsymbol{k}}$ as

$$|M(\varepsilon_{n\boldsymbol{k}})| = \left(\frac{\sum_{m\boldsymbol{k}'} |M_{mn}(\boldsymbol{k}', \boldsymbol{k})|^2 \delta(\varepsilon_{m\boldsymbol{k}'} - \varepsilon_{n\boldsymbol{k}})}{\sum_{m\boldsymbol{k}'} \delta(\varepsilon_{m\boldsymbol{k}'} - \varepsilon_{n\boldsymbol{k}})} \right)^{1/2}, \tag{S2}$$

where $M_{mn}(\boldsymbol{k}', \boldsymbol{k})$ is the e-d matrix element coupling Bloch state $|n\boldsymbol{k}\rangle$ to $|m\boldsymbol{k}'\rangle$. This quantity has contributions from all the final scattering states $|m\boldsymbol{k}'\rangle$ and can quantify the scattering strength for a carrier with energy $\varepsilon_{n\boldsymbol{k}}$. Supplementary Figure 2 shows this e-d scattering strength for vacancy defects in copper (upper panel) and silicon (lower panel). In copper, the scattering strength for a 1 ppm vacancy concentration is of order 30-50 eV for states near the Fermi energy, versus a much lower value of about 5 eV in silicon for states near the valence band edge. This result shows quantitatively that electron-vacancy scattering is stronger in copper than in silicon.

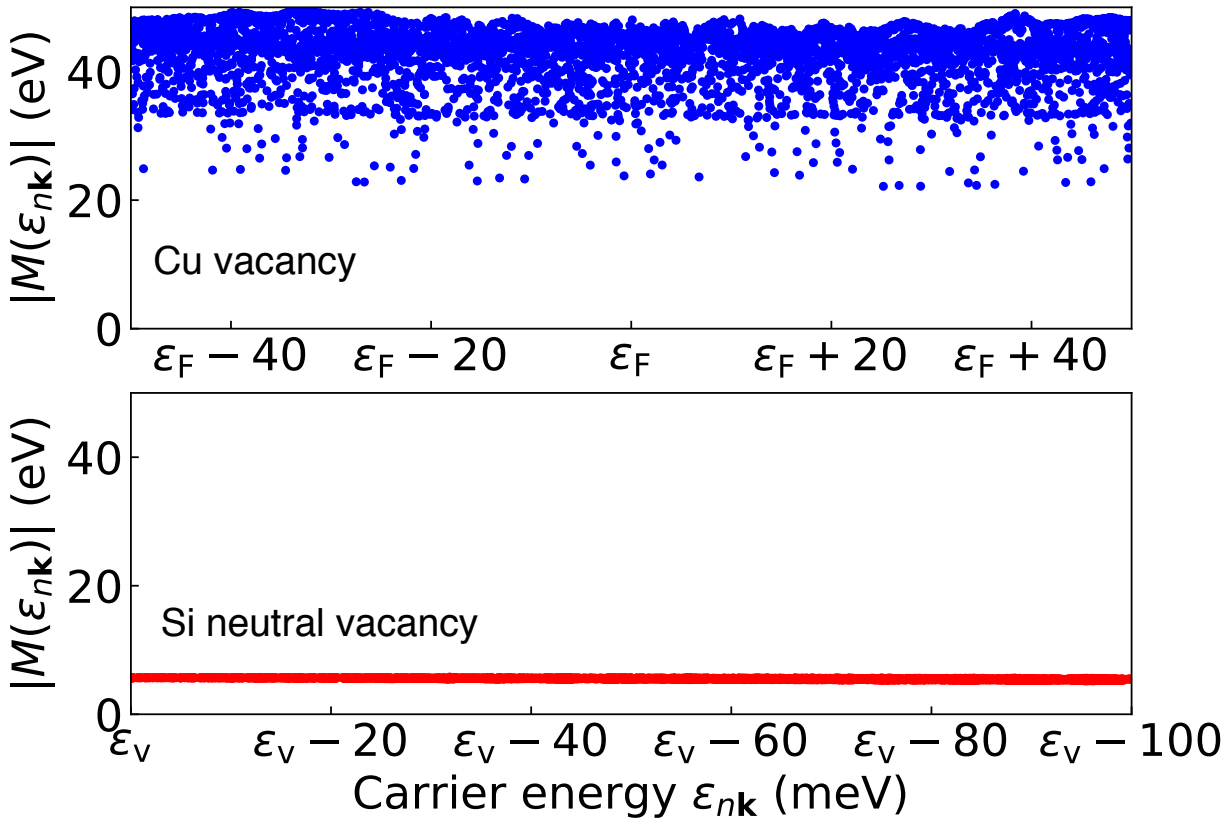

Supplementary Figure 2. Scattering strength in copper (upper panel) and silicon (lower panel) for vacancy defects as a function of carrier energy. For copper, we show the scattering strength for electronic states within 50 meV of the Fermi energy ε_F, and in silicon for states within 100 meV of the valence band maximum ε_v. To compute the scattering strength in Eq. (S2), we use a fine BZ grid with 240^3 $\boldsymbol{k}_f$-points, starting from coarse BZ grids with 10^3 $\boldsymbol{k}_c$-points for silicon and 8^3 $\boldsymbol{k}_c$-points for copper.